Ultimate Capacity of Structural Steel Cross Section under Compression, Bending and Combined Loading

Jyoti[1], Rachna [2] , Satish Kumar [3], Jaidutt[4]
[1,2,3,4]Department of Civil Engineering,
Applied college of Management & Engineering,
Palwal Haryana, India

***Abstract*- The Continuous Strength Method (CSM) is a strain based structural steel design approach which allows for the beneficial influence of strain hardening. The method has been previously developed for predicting compression and bending resistances in isolation. This paper describes extension of the method to enable the prediction of the ultimate cross-section resistance of I-sections and box sections under combined loading. At the core of the method is a base curve, which relates the deformation capacity of a cross-section to its cross-section slenderness. Deformation capacity is defined as the ratio of the maximum strain that a cross-section can endure relative to its yield strain. Knowing this limiting strain and assuming plane sections remain plane, the resistance of a cross-section to combinations of axial load and bending moments can be calculated, by integrating the stresses arising from a suitable strain hardening material model over the area of the cross-section. By considering a range of combinations of applied actions, analytical expressions and numerically derived interaction surfaces have been produced, which were then rationalised into simple expressions for use in design. The resulting CSM design predictions for box sections and I-sections have been compared with existing test data, and shown to give additional capacity over current design approaches and a reduction in scatter of the predictions.**

Keywords*- *Compression; Bending; Combined loading; Steel structures; Strain hardening; Continuous Strength Method

I. INTRODUCTION

Design rules for structural steel cross-sections often include simplifications that allow quick and conservative estimates of capacity (e.g. the ability to withstand combinations of axial forces, shear forces and bending moments) to be obtained. Some of these simplifications are at the material level, where structural steel is typically assumed to have an elastic–plastic or rigid–plastic stress–strain ($\sigma - \epsilon$) response, some are based on equations limited by elastic conditions, while other approximations involve the grouping of similar behaviour, as in the case of cross-section classification for the treatment of local buckling.

At the ultimate limit state, a cross-section subjected to flexure is typically designed on the basis of its plastic ($M_{pl} = W_{pl}f_y$) or elastic moment capacity ($M_{el} = W_{el}f_y$), where W_{pl} and W_{el} are the plastic and elastic section moduli and f_y is the material yield stress. The choice between the two is based on the susceptibility of the cross-section to local buckling, which is assessed by considering the width-to-thickness ratios of the elements that make up the cross-section through a process known as cross-section classification. For slender cross-sections, where local buckling occurs prior to the initiation of yielding, reduced moment capacities are assigned. This approach generally results in a step from M_{el} to M_{pl} at a particular slenderness limit.

II. MATERIAL MODEL

The stress–strain ($\sigma - \epsilon$) response of structural steel can differ depending on the material grade and how the material has been manufactured, subsequently mechanically worked, and ultimately tested. Hot-rolling (Fig. 1a) or cold-forming (Fig. 1b) can affect the material behaviour by altering the distinctiveness of the yield point, the length of the yield plateau, and the magnitude of the strain hardening slope. Variation in material properties around structural cross-sections is also possible, such as in the case of cold-formed sections, where higher strength but lower ductility are typically found in the corner regions..

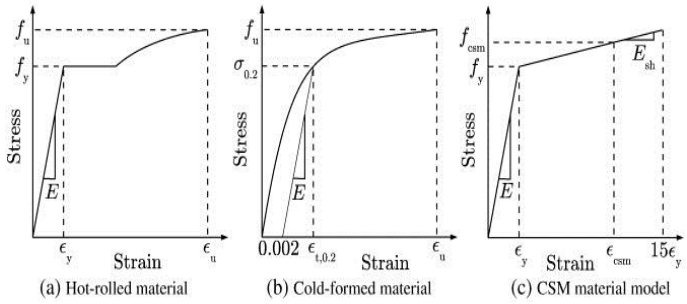

Fig. 1. Schematic stress–strain curves (a) for hot-rolled material, (b) cold-formed material and (c) the CSM material model.

In Fig. 1, E is the Young's modulus, f_y and f_u are the yield and ultimate tensile stresses, $\epsilon_y = f_y/E$ and ϵ_u are the strains at the yield and ultimate stress, $\sigma_{0.2}$ and $\epsilon_{t,0.2}$ are the 0.2% offset proof stress and corresponding strain, E_{sh} is the strain hardening slope and f_{csm} and ϵ_{csm} are the CSM limiting stress and strain. Traditionally a bi-linear, elastic–perfectly plastic material model is used to model structural steel, with the key advantage of being very simple to analyse, but with the potential disadvantage of being overly conservative since no post-yield strain hardening is accounted for. Alternatives to the elastic–perfectly plastic

model include bi-linear (elastic–linear hardening), tri-linear, power, Ramberg and Osgood and other stress–strain models. In principle, any material law can be used in conjunction with the deformation based CSM. The proposed material model (Fig. 1c) is an elastic–linear hardening relationship, which consists of an initial linear region with Young's modulus E defining stresses up to the yield stress, followed by a strain hardening region, described by an appropriate strain hardening modulus E_{sh} for the material. A maximum limiting strain is also set at 15 times the yield strain ($\epsilon_{csm}/\epsilon_y = 15$), a value which corresponds to the material ductility requirements given in Clause 3.2.2(1) of EN 1993-1-1. This material model gives the following stress–strain relationship:

equation(1)

$$\sigma = \begin{cases} E\epsilon & \epsilon \le \epsilon_y \\ f_y + E_{sh}(\epsilon - \epsilon_y) & \epsilon_y < \epsilon \le \epsilon_{csm} \end{cases}$$

σ=Eϵϵ≤ϵyfy+Eshϵ−ϵyϵy<ϵ≤ϵcsm.

The key characteristic to be defined in the adopted material model is the strain hardening modulus E_{sh}, which should be representative of the whole cross-section.

III. CROSS- SECTION SLENDERNESS

Local plate buckling may initiate before or after the onset of material yielding, with the key determining geometric factor being the relative width-to-thickness ratios of the plate elements that make up the cross-section. Plate slenderness is commonly defined in the non-dimensional form of equation(2)

$$\bar{\lambda}_p = \sqrt{\frac{f_y}{\sigma_{cr}}}$$ λ¯p=fyσcr

where σ_{cr} is the elastic buckling stress, which is influenced by the boundary and loading conditions of the plate. The plate slenderness values of all the elements that make up the cross-section are evaluated, with the critical and governing element determined as that with the highest value of $\bar{\lambda}_p$ λ¯p. Since basing the cross-section slenderness upon the most slender constituent plate element does not consider the connectivity between the plates.Cross-section slenderness reduces when element interaction is considered; this reduction is by a factor of between 0.85–1.0 for axial loading, and approximately 0.70–1.0 for major or minor axis bending for typical hot-rolled structural profiles

IV. STRAIN RATIO AND CURVATURE RATIO

The CSM is a deformation based design approach, founded upon a derived relationship between the failure strain of a cross-section and its local slenderness. The results of both stub column and in-plane bending tests can be used in the derivation of this relationship. A stub column is defined herein as a column with a global non-dimensional slenderness $\bar{\lambda} \le 0.1$ λ¯≤0.1, where $\bar{\lambda} = \sqrt{N_y/N_{cr}}$ λ¯=Ny/Ncr, N_y being the yield load of the cross-section and N_{cr} the elastic buckling load of the member. While meeting the above requirement of $\bar{\lambda} \le 0.1$ λ¯≤0.1 to avoid any significant influence from global buckling, the test lengths L of stub columns should also ideally be at least three times the larger cross-sectional dimension, in order to contain a representative distribution of geometric imperfections and residual stresses and to allow local failure modes to form without a strong influence from end effects.A typical load–end-shortening ($N - \delta$) curve from a stub column test is shown in Fig. 2, where loads above the yield load will be reached if the cross-section slenderness is sufficiently low to allow stresses to enter the strain hardening regime. The end-shortening δ at the ultimate load N_{lb} (i.e. the peak load N_u achieved in the stub column test), is divided by the length of the specimen to obtain the average failure strain of the cross-section ϵ_{lb}. The deformation capacity of the stub column is then defined as ϵ_{csm}, which is taken directly as ϵ_{lb} for materials that exhibit a distinct yield point and as $\epsilon_{lb} - 0.002$ for materials with a rounded stress–strain curve. The subtraction of 0.2% strain in the case of rounded stress–strain curves is to ensure compatibility with the chosen material model of Fig. 1c and to avoid over-predictions of capacity. The CSM strain is normalised by the yield strain in Eqn. (3), and $\epsilon_{csm}/\epsilon_y$ is referred to as the strain ratio.

equation(3)

$$\frac{\epsilon_{csm}}{\epsilon_y} = \begin{cases} \frac{\epsilon_{lb}}{\epsilon_y} & \text{for hot-rolled materials with distinct yield point} \\ \frac{\epsilon_{lb}-0.002}{\epsilon_y} & \text{for cold-formed and non-linear materials.} \end{cases}$$

ϵcsmϵy=ϵlbϵyforhot-rolledmaterialswithdistinctyieldpointϵlb−0.002ϵyforcold-formedandnon-linearmaterials.

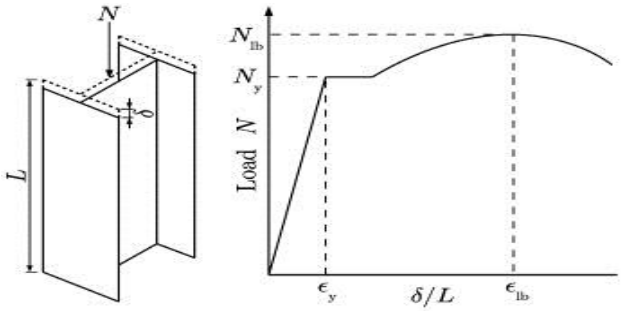

Fig. 2. Stub column load–deformation response.

Cross-sections that fail at strain ratios greater than unity can exceed their yield loads and mobilise some of their strain hardening potential. Note that, in the present study, when considering test specimens that exhibit a variation in material properties around the cross-section (e.g. enhanced strength at corners due to cold-forming), area weighted average values have been used to establish N_y and ϵ_y. For slender cross-sections (defined herein as cross-sections with $\bar{\lambda}_p > 0.68$ λ¯p>0.68), elastic local buckling is followed by stable post-buckling, which results in increased capacities but with reduced axial stiffness. The consequence of this is that a slender cross-section can have a high deformation capacity (i.e. strain at failure), greater than ϵ_y, but a peak load still below the yield load. This would result in an over-prediction of capacity when using

the CSM. To avoid this, the deformation capacity of slender cross-sections is defined by Eqn. (4).

equation(4)

$$\frac{\epsilon_{csm}}{\epsilon_y} = \frac{N_u}{N_y} \quad \text{for} \quad \frac{N_u}{N_y} < 1 \quad \text{or} \quad \overline{\lambda}_p > 0.68.$$

ϵcsmϵy=NuNyforNuNy<1orλ¯p>0.68.

The value of $\overline{\lambda}_p = 0.68$ λ¯p=0.68 has been found by Afshan and Gardner to represent the transition point for which cross-sections behave as either slender (achieving peak loads below the yield values N_y and M_{el}), or as non-slender (achieving peak loads above the yield values). For cross-sections in bending, the strain distribution is assumed to be linearly-varying through the cross-section depth, and a relationship can be made between curvature and outer-fibre strains. With the height and width of a cross-section denoted as h and b, the yield curvatures $\kappa_{y,y}$ and $\kappa_{y,z}$ for the major and minor axes are defined as:

equation(5)

$$\kappa_{y,y} = \frac{2\epsilon_y}{h} \quad \text{and} \quad \kappa_{y,z} = \frac{2\epsilon_y}{b}.$$

κy,y=2ϵyhandκy,z=2ϵyb.

These are the curvatures at which a cross-section will reach its major and minor axis elastic moments, $M_{el,y}$ and $M_{el,z}$ respectively. Assuming that plane sections remain plane during bending, there is a proportional relationship between the strains at $\pm h / 2$ and $\pm b / 2$ and curvature. This permits the equivalence of the strain ratio $\epsilon_{csm}/\epsilon_y$ to the curvature ratio κ_{csm}/κ_y, where κ_{csm} is the curvature when the strain ϵ_{csm} is reached in the outer-most compressive outer-fibre of the cross-section.

equation(6)

$$\frac{\kappa_{csm}}{\kappa_y} = \begin{cases} \frac{\kappa_{lb}}{\kappa_y} & \text{for hot-rolled materials with distinct yield point} \\ \frac{\kappa_{lb} - \frac{0.002}{h/2}}{\kappa_y} & \text{for cold-formed and non-linear materials} \end{cases}$$

in which κ_{lb} is the curvature at maximum moment M_{lb} (or M_u). Hence κ_{csm} is related to κ_{lb} in a similar manner to the relationship between ϵ_{csm} and ϵ_{lb}, as defined by Eqn. (6) for the case of the major axis. For slender cross-sections ($\overline{\lambda}_p > 0.68$ λ¯p>0.68) in bending, the definition of curvature ratio, given by Eqn. (6) has been modified for similar reasons to those previously explained for compression:

equation(7)

$$\frac{\kappa_{csm}}{\kappa_y} = \frac{M_u}{M_{el}} \quad \text{for} \quad \frac{M_u}{M_{el}} < 1 \quad \text{or} \quad \overline{\lambda}_p > 0.68.$$

κcsmκy=MuMelforMuMel<1orλ¯p>0.68.

This allows experimental bending data to be plotted on a common deformation capacity–slenderness curve with axial test data;

V. BASE CURVE

The CSM base curve relates normalised cross-section failure strain $\epsilon_{csm}/\epsilon_y$ to cross-section slenderness $\overline{\lambda}_p$ λ¯p. Stub column test data were collected for specimens that had been tested to failure,; the majority of the test cross-sections were non-slender and had therefore reached axial loads and strains above the yield values, N_y and ϵ_y. In addition, test data on short or laterally restrained beams in four-point bending, and were also collated. These data are plotted in Fig. 3 on a graph of strain ratio versus cross-section slenderness, alongside equivalent stainless steel and and aluminium and test data.

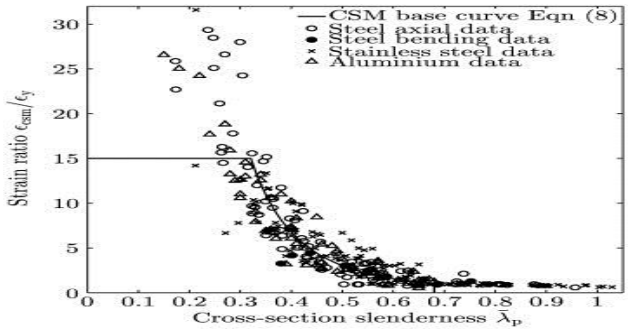

Fig. 3. CSM base curve with stub column and bending test data for structural steel, stainless steel and aluminium.

The test data shows a clear trend of increasing deformation capacity with reducing cross-section slenderness (i.e. lower $\overline{\lambda}_p$ λ¯p), with the strain at peak load sometimes exceeding $25\epsilon_y$. For the slender cross-sections ($\overline{\lambda}_p > 0.68$ λ¯p>0.68), the strain ratio drops below the elastic value of $\epsilon_{csm}/\epsilon_y = 1$. A non-linear least squares fit to the collected data set, excluding cross-sections where $\overline{\lambda}_p > 0.68$ λ¯p>0.68, is given by Eqn. (8), with an upper bound of 15 applied to the strain ratio to avoid excessive strains and to remain within the fracture ductility limits set out in EN 1993-1-1. Fig. 3 shows a good match between the collected test data and Eqn. (8). Similar agreement was observed between a slightly modified version of Eqn. (8) by [9] and the numerical results for a range of material models. Hence, Eqn. (8), referred to as the CSM base curve, may be used to predict the CSM failure strain ϵ_{csm} from the cross-section slenderness $\overline{\lambda}_p$ λ¯p.

equation(8)

$$\frac{\epsilon_{csm}}{\epsilon_y} = \frac{0.25}{\overline{\lambda}_p^{3.6}} \quad \text{but} \quad \frac{\epsilon_{csm}}{\epsilon_y} \leq 15$$

ϵcsmϵy=0.25λ¯p3.6butϵcsmϵy≤15

VI. AXIAL AND BENDING RESISTANT

A. AXIAL RESISTANT

For a column unaffected by global buckling, the strains in the cross-section are assumed to be uniform at ϵ_A. When $\epsilon_A < \epsilon_y$, the cross-section is within its elastic material range. However, when $\epsilon_A \geq \epsilon_y$ the cross-section is deforming inelastically and, following the CSM strain hardening material model described in Section 2.1, will reach the CSM limiting stress f_{csm}. Thus, for $\epsilon_{csm}/\epsilon_y > 1$, the CSM axial resistance N_{csm} given by Eqn. (9), will be greater than the yield load. In Eqn. (9), γ_{M0} is the partial factor for

cross-section resistance, with a recommended value of unity.

equation(9)

$$N_{csm} = \frac{A f_{csm}}{\gamma_{M0}} \quad \text{with} \quad f_{csm} = f_y + E_{sh}\left(\epsilon_{csm} - \epsilon_y\right)$$ Ncsm=Afc smγM0withfcsm=fy+Eshϵcsm−ϵy

B. BENDING CAPACITY

In bending, a cross-section that has a strain ratio equal to unity will have an outer-fibre stress equal to the yield stress, and will fail at the elastic moment capacity M_{el}. For higher strain ratios, the outer-fibre CSM stress f_{csm} will be greater than the yield stress f_y, and the cross-section resistance will exceed the elastic moment capacity. This results from the fact that the integrals $M_{csm,y} = \int \sigma y \, dA$ and $M_{csm,z} = \int \sigma z \, dA$, where stresses are defined from a linear strain distribution and the CSM bi-linear material model, and y and z are the distances from the neutral axes, will result in moments greater than M_{el}. Cross-sections with higher $\epsilon_{csm}/\epsilon_y$ enter further into the strain hardening regime and can achieve $M_{csm} > M_{pl}$.For the cross-section geometry shown in Fig. 4, an analytical moment resistance expression was presented by [9], which gave the normalised moment capacity of Eqn. (10), where the appropriate section moduli $W_{pl,y}$ and $W_{el,y}$ or $W_{pl,z}$ and $W_{el,z}$ are used for bending about the y–y or z–z axes.

equation(10)

$$\frac{M_{csm}}{M_{pl}} = 1 + \frac{E_{sh}}{E}\left(\frac{\epsilon_{csm}}{\epsilon_y}\frac{W_{el}}{W_{pl}} - 1\right) - \frac{W_w}{W_{pl}}\left(1 - \frac{E_{sh}}{E}\right)$$ McsmMpl =1+EshEϵcsmϵyWelWpl−1−WwWpl1−EshE

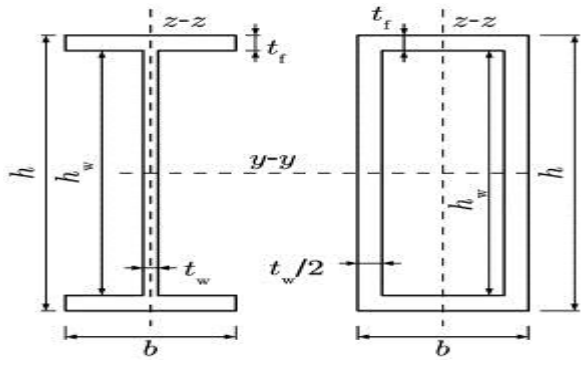

Fig. 4. For box and I-sections bending about the major axis, the W_w modulus is defined by Eqn. (11):

equation(11)

$$W_w \begin{cases} \frac{t_w h^2}{12}\left(\frac{\epsilon_{csm}}{\epsilon_y}\right)^{-2} & \text{for } 1 + \frac{2t_f}{h_w} \le \frac{\epsilon_{csm}}{\epsilon_y} \\ \frac{bh^2}{12}\left(\frac{\epsilon_{csm}}{\epsilon_y}\right)^{-2} - \frac{(b-t_w)}{12}h_w^2\left(3 - \frac{2h_w}{h}\frac{\epsilon_{csm}}{\epsilon_y}\right) & \text{for } 1 + \frac{2t_f}{h_w} > \frac{\epsilon_{csm}}{\epsilon_y} \ge 1 \end{cases}$$

Wwtwh212ϵcsmϵy−2for1+2tfhw≤ϵcsmϵybh212ϵcsmϵy−2−b−tw12hw23−2hwhϵcsmϵyfor1+2tfhw>ϵcsmϵy≥1.

For box sections bending about the minor axis, the W_w modulus in Eqn. (12) is similar to Eqn. (11):

equation(12)

$$W_w = \begin{cases} \frac{t_w b^2}{12}\left(\frac{\epsilon_{csm}}{\epsilon_y}\right)^{-2} & \text{for } \frac{1}{1 - \frac{t_w}{b}} \le \frac{\epsilon_{csm}}{\epsilon_y} \\ \frac{hb^2}{12}\left(\frac{\epsilon_{csm}}{\epsilon_y}\right)^{-2} - \frac{h - t_w}{12}(b - t_w)^2\left[3 - 2\left(1 - \frac{t_w}{b}\right)\frac{\epsilon_{csm}}{\epsilon_y}\right] & \text{for } \frac{1}{1 - \frac{t_w}{b}} > \frac{\epsilon_{csm}}{\epsilon_y} \ge 1 \end{cases}$$

Ww=twb212ϵcsmϵy−2for11−twb≤ϵcsmϵyhb212ϵcsmϵy−2−h−tw12b−tw23−21−twbϵcsmϵyfor11−twb>ϵcsmϵy≥1.

I-sections perform notably different about the minor axis and have modulus W_w as:

equation(13)

$$W_w = \begin{cases} \frac{hb^2}{12}\left(\frac{\epsilon_{csm}}{\epsilon_y}\right)^{-2} & \text{for } \frac{\epsilon_{csm}}{\epsilon_y} \ge \frac{b}{t_w} \\ \frac{t_w^2 h_w}{2}\left(\frac{1}{2} - \frac{t_w}{3b}\frac{\epsilon_{csm}}{\epsilon_y}\right) + \frac{t_f b^2}{6}\left(\frac{\epsilon_{csm}}{\epsilon_y}\right)^{-2} & \text{for } \frac{\epsilon_{csm}}{\epsilon_y} < \frac{b}{t_w} \end{cases}$$

Ww=hb212ϵcsmϵy−2forϵcsmϵy≥btwtw2hw212−tw3bϵcsmϵy+tfb26ϵcsmϵy−2forϵcsmϵy<btw.

The analytical equations are exact for the chosen bi-linear material model, but are lengthy for practical design due to the W_w term. However, accurate approximations to Eqns. (11), (12) and (13) are achieved using the simpler design expression of Eqn. (14):

$$M_{csm} = \frac{W_{pl} f_y}{\gamma_{M0}}\left[1 + \frac{E_{sh}}{E}\frac{W_{el}}{W_{pl}}\left(\frac{\epsilon_{csm}}{\epsilon_y} - 1\right) - \left(1 - \frac{W_{el}}{W_{pl}}\right) \Big/ \left(\frac{\epsilon_{csm}}{\epsilon_y}\right)^{\alpha}\right]$$

Mcsm=WplfyγM01+EshEWelWplϵcsmϵy−1−1−WelWpl/ϵcsmϵyα

where $\alpha = 2$ for I-sections bending about the major axis and box sections bending about either axis, and $\alpha = 1.2$ for I-sections bending about the minor axis. This CSM design bending equation requires the assignment of three ratios to the cross-section: the ratio of strain hardening modulus to Young's modulus E_{sh}/E, the shape factor reciprocal W_{el}/W_{pl}, and the strain ratio $\epsilon_{csm}/\epsilon_y$.

VII. COMBINED AXIAL LOAD AND BENDING

Combined loading differs from the basic cases of axial load or uni-axial bending in that stresses and strains depend on both the y and z coordinates (i.e. those in the plane of the cross-section). The proposed CSM model for doubly symmetric cross-sections under combined loading is based on orientations of a rotated (due to bending) planar strain surface shifted by a uniform compressive strain ϵ_A and limited by the CSM strain ϵ_{csm}. Examples of such strain planes are shown in Fig. 5, from which the stresses and cross-section resistances to axial forces and bending moments may be derived; this is undertaken by means of a numerical model, as described in Section 4.2.

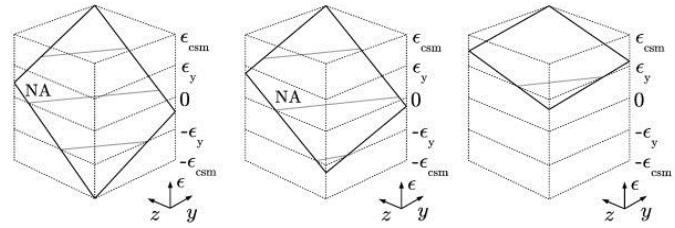

(a) No compressive strain ϵ_A (b) Low compressive strain ϵ_A (c) High compressive strain ϵ_A

Fig. 5. Strain distributions in cross-sections under combined axial load and bi-axial bending; compression is positive and NA is the neutral axis.

For bending about both axes and with $\epsilon_A = 0$ (Fig. 5a), the area and distribution of stresses in compression equal those in tension and no net axial force is produced; when ϵ_A is non-zero a net axial force exists. Failure of the cross-section is deemed to occur when the maximum compressive strain reaches the CSM limiting strain ϵ_{csm}. With reference to Fig. 5, the maximum compressive strain will occur at $y = h/2$, $z = b/2$ for box and I-sections. The uniform compressive strain ϵ_A has the effect of preventing the tensile corner strain (at $y = -h/2$, $z = -b/2$) from reaching $-\epsilon_{csm}$ and accelerating the compressive corner strain reaching ϵ_{csm} (Fig. 5b and Fig.5c).

VIII. NUMERICAL MODEL

In this subsection, cross-section capacities under combined loading are determined by means of a numerical model. In the numerical model, the cross-section is divided into i elements each of area A_i, and with element centroids at distances y_i and z_i from the centroidal axes of the cross-section. There are three strain components that must be considered: ϵ_A, ϵ_B and ϵ_C. The strain ϵ_A is the uniform strain across the whole of the cross-section, associated with axial deformations. The strains ϵ_B and ϵ_C describe bending about the major and minor axes respectively. The linearly varying strains are associated with flexural deformations and are defined by $2y_i\epsilon_B/h$ for the major axis and $2z_i\epsilon_C/b$ for the minor axis. The numerical analysis procedure is initiated with a given value of $\epsilon_A/\epsilon_{csm}$ from between 0 and 1, with $\epsilon_A = 0$ indicating no axial deformations and $\epsilon_A = \epsilon_{csm}$ indicating only axial loading. The parameter $\epsilon_B/\epsilon_{csm}$ is then varied from 0, for no major axis bending, to $1 - \epsilon_A/\epsilon_{csm}$ for axial load plus major axis bending. This limits the maximum value of the minor axis bending parameter $\epsilon_C/\epsilon_{csm} = 1 - \epsilon_A/\epsilon_{csm} - \epsilon_B/\epsilon_{csm}$. The strain ϵ_i at element i is then given by Eqn. (15), based on the addition of ϵ_A, ϵ_B and ϵ_C, all normalised by ϵ_{csm}. equation(15)

$$\frac{\epsilon_i}{\epsilon_{csm}} = \frac{\epsilon_A}{\epsilon_{csm}} + \frac{\epsilon_B}{\epsilon_{csm}}\frac{2y_i}{h} + \left(1 - \frac{\epsilon_A}{\epsilon_{csm}} - \frac{\epsilon_B}{\epsilon_{csm}}\right)\frac{2z_i}{b}$$ ϵiϵcsm=ϵAϵcsm+ϵBϵcsm2yih+1−ϵAϵcsm−ϵBϵcsm2zib

The failure criterion is based on $2y_i/h = 2z_i/b = 1$, that is the CSM limiting strain ϵ_{csm} being reached at the corner element where $y_i = h/2$, $z_i = b/2$, and $\epsilon_A + \epsilon_B + \epsilon_C = \epsilon_{csm}$. As ϵ_A increases, the strain plane can rotate to a lesser extent before ϵ_{csm} is reached and hence the lower the capacity of the cross-section to co-existing bending (corresponding to lower values of ϵ_B and ϵ_C). With the strain at each element known, the element stress f_i normalised by the yield stress is calculated from Eqn. (16).

equation(16)

$$\frac{f_i}{f_y} = \begin{cases} \dfrac{\epsilon_i}{\epsilon_y} & \epsilon_i \le \epsilon_y \\ 1 + \dfrac{E_{sh}}{E}\left(\dfrac{\epsilon_i}{\epsilon_y} - 1\right) & \epsilon_i > \epsilon_y \end{cases}$$ fify=ϵiϵyϵi≤ϵy1+EshEϵiϵy−1ϵi>ϵy

The normalised cross-section resistances N (axial force), M_y (major axis bending) and M_z (minor axis bending) are then:

equation(17)

$$\frac{N}{N_y} = \frac{1}{A}\sum_i \frac{f_i}{f_y}A_i$$ NNy=1A∑ififyAi

equation(18)

$$\frac{M_y}{M_{pl,y}} = \frac{1}{W_{pl,y}}\sum_i \frac{f_i}{f_y}y_iA_i$$ MyMpl,y=1Wpl,y∑ififyyiAi

equation(19)

$$\frac{M_z}{M_{pl,z}} = \frac{1}{W_{pl,z}}\sum_i \frac{f_i}{f_y}z_iA_i.$$ MzMpl,z=1Wpl,z∑ififyziAi.

The output from the numerical model is a suite of interaction curves between M_y and M_z, as displayed in Fig. 6 for an I-section with a strain ratio of 15. This forms an interaction surface that can be used to create design interaction curves for different combinations of axial load and bending moments. The curves and surfaces can be plotted in two or three-dimensional space with respect to the plastic resistances $M_{pl,y}$, $M_{pl,z}$ and N_y or, more suitably, with respect to the CSM resistances $M_{csm,y}$, $M_{csm,z}$ and N_{csm}.

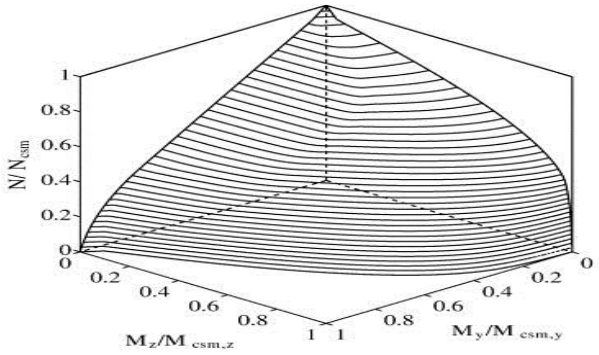

Fig. 6. Typical interaction surface generated from the numerical model for an I-section with a strain ratio $\epsilon_{csm}/\epsilon_y = 15$.

The numerically generated surfaces can be used to create interaction curves between major axis and minor axis bending for a given axial load, and for a constant strain ratio. This gives contours of constant axial load by slicing through the interaction surface with a series of parallel planes. Examples of these contours with curves normalised by the plastic moment capacities, are displayed in Fig. 7 and Fig. 8 for a typical I-section and box section respectively, both of which have a strain ratio of 15 and are

plotted with and without strain hardening ($E_{sh} = E/100$ and $E_{sh} = 0$). curves provide a good representation of the numerically generated results for the case of no strain hardening, though some deviation may be seen in the middle region of the I-section curves. It may also been seen that as the axial load increases, the bi-axial bending interaction curves from both the numerical model and EN 1993-1-1 contract towards the origin and become more rectangular in shape. The influence of strain hardening, which is essentially to expand the interaction surfaces, may also be clearly seen from the numerical results. In the following subsection, design interaction expressions are developed on the basis of the numerical results.

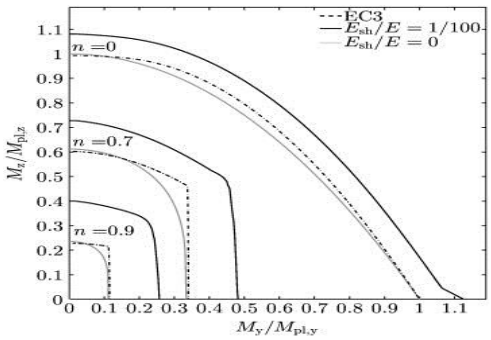

Fig. 7. Bi-axial bending interaction curves for a typical I-section at fixed axial load levels $n = N/N_y$.

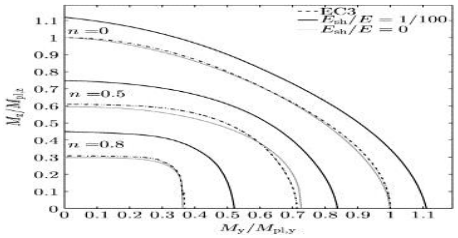

Fig. 8.Bi-axial bending interaction curves for a typical box section at fixed axial load levels $n = N/N_y$.

IX. DESIGN INTERACTION CURVE

This subsection introduces the CSM design equation for combined loading, shows comparisons with the numerical model presented in Section 4.2, and defines a goodness of fit by a residual. The proposed design equations for the prediction of the combined axial load and bending capacity of a cross-section, are based on curve fits that rationalise the numerical model surface in the CSM domain. In CSM normalised space, the surfaces are bound to a unit box defined by $M_{csm,y}$, $M_{csm,z}$ and N_{csm}; this prevents the interaction surfaces from progressively expanding outwards away from the origin as the strain ratio (and hence cross-section capacity) increases.The proposed form of design equations, given by Eqns. (20) and (21), trace bi-axial bending interaction curves that are anchored by reduced moments $M_{R,csm,y}$ and $M_{R,csm,z}$, which are functions of the axial load level $n = N/N_{csm}$. Eqn. (20) contains two reduced moment normalised terms for major and minor axis bending, raised to powers α and β respectively.The equations provide smooth curves between $M_{R,csm,y}$ and $M_{R,csm,z}$, and map surfaces that conform well to the numerical model surfaces.equation(20)

$$\left(\frac{M_y}{M_{R,csm,y}}\right)^{\alpha} + \left(\frac{M_z}{M_{R,csm,z}}\right)^{\beta} \leq 1$$

MyMR,csm,yα+MzMR,csm,zβ≤1

equation(21)

$$M_{R,csm,y} = M_{csm,y}\left(1-n^{a_y}\right)^{\frac{1}{b_y}} \quad \text{and} \quad M_{R,csm,z} = M_{R,csm,z}\left(1-n^{a_z}\right)^{\frac{1}{b_z}}$$

MR,csm,y=Mcsm,y1−nay1byandMR,csm,z=Mcsm,z1−naz1bz

The design equations simplify when the appropriate loading terms are taken as zero. For example, when there is no axial load ($n = 0$), the reduced moments in Eqn. (21) collapse to the CSM moments and convert Eqn. (20) into a bi-axial bending design equation, and when either M_y or M_z is zero, the equations collapse into the simple axial load and uni-axial bending forms of $M_z \leq M_{R,csm,z}$ and $M_y \leq M_{R,csm,y}$ respectively.The powers a_y, a_z, b_y, b_z, α and β are all defined in Table 1. The tabulated powers were found via a non-linear least squares fitting regime, and are based on the ratio of the cross-section web area to gross area $a = A_w/A$ and the ratio of the major to minor axis plastic section moduli $W_r = W_{pl,y}/W_{pl,z}$. A strain ratio of 5 is required before the convergence of the powers for I-sections, compared to that of 3 needed for box sections. The powers a_y, a_z, b_y, b_z, α and β are all unity when $\epsilon_{csm}/\epsilon_y < 3$.

.

α	$2 - 1.5n \geq 1$	$2 + 0.15W_r - 5n^{1.5} \geq 1.3$	$1.75 + W_r(2n^2 - 0.15) \leq 1.7 + W_r$
β	$0.8 + 5n^{2.2} \leq 4$	$0.8 + (15 - W_r)n^{2.2} \leq 8$	$1.6 + (3.5 - 1.5W_r)n^2 \leq 3.7 - W_r$

The CSM design equation for a typical I-section (for strain ratios 5–15) and box section (for strain ratios 3–15) are plotted in Fig. 9 and Fig. 10 respectively, together with the corresponding numerical envelopes. For both cross-sections, the design equations fit well to the numerical model, providing interaction curves that pass through the middle of the envelopes, or giving predictions on the conservative side. For the I-section, the straight sides of the curves at high axial loads are produced by the larger β powers.

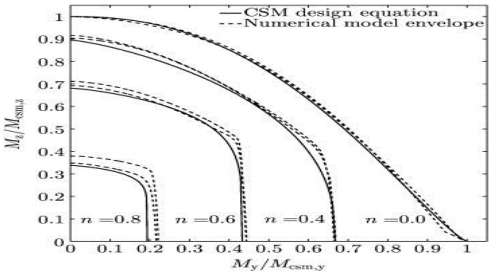

Fig. 9. I-section numerical model envelopes (strain ratios 5–15) and the CSM design equation for combined loading.

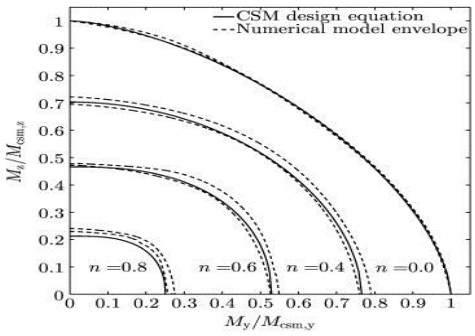

Fig. 10. Rectangular hollow section numerical model envelopes (strain ratios 3–15) and the CSM design equation for combined loading.

In order to assess the conformity between the design interaction surfaces and the numerical results, a residual is defined. The selected residual definition is the distance between the design interaction surfaces produced by Eqns. (20) and (21) and an associated point produced by the numerical model, based on a projection from the origin to the surface. The line from the origin to the known numerical data point *R*, will intersect the trial surface at point S, with the distance from the origin to this intersection as $S=cR$. The scalar c for every interaction surface point is then found by solving implicitly by a numerical root finding procedure, and the residual is then expressed as $100(1-c)$ %. A positive value of the residual corresponds to the numerical point lying outside the design interaction surface and therefore a conservative prediction of capacity. For a negative value, the opposite is true.

Fig. 11 and Fig. 12 show shaded surface maps of the residuals for a typical I-section and box section respectively. For the I-section, the magnitudes of the residuals are less than 3.5%, with a negative region appearing towards the centre of the surface, and two smaller concentrations at the $M_{csm,y}$ and N_{csm} end points. The shaded residual plot is more uniform for the box section and gives residuals of lower magnitude, the highest being approximately 2.5%. A similar residual analysis based on the EN 1993-1-1 combined loading equations, but using the CSM axial and moment capacities in place of the yield load and plastic moment capacities, leads to residuals which are on average 1–2% greater in magnitude than the CSM design equations using the powers.

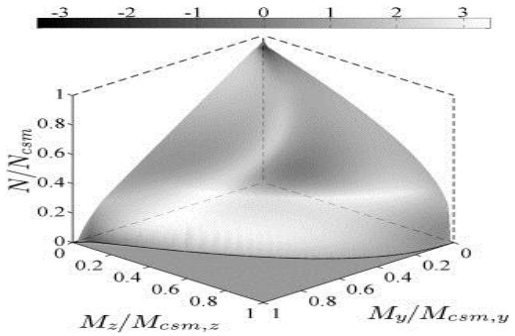

Fig. 11. I-section residuals (%) between the CSM design equation and the numerical results (strain ratio of 15).

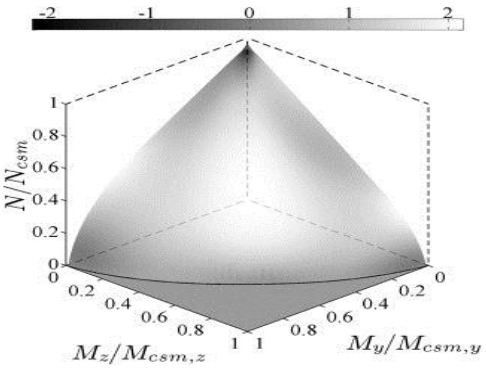

Fig. 12. Rectangular hollow section residuals (%) between the CSM design equation and the numerical results (strain ratio of 15)

X. CONCLUSION

The Continuous Strength Method (CSM) is a strain based structural design approach that has been previously developed for cross-sections under either compression or bending. Herein, the method was extended to the case of combined loading. Analyses have been performed for structural steel I-sections and box sections via a strain based numerical model, and rationalised with simple equations suitable for use in design.

A bi-linear material model was represented that combined the stress–strain relationships of hot-rolled and cold-formed structural steel and allowed for the benefits of strain hardening. A maximum strain of 15 times the yield strain was allowed based upon ductility requirements, and a value of $E_{sh} = E/100$ was selected to represent the strain hardening modulus. A strain ratio and curvature ratio were defined as the strain or curvature at the peak axial load or peak bending moment from tests, and then normalised by the yield values. Higher values of strain ratio indicated greater deformation capacity and hence increased resistance to local buckling. The relationship between the strain ratio and the cross-section slenderness was displayed on a base curve, for which a suitable expression was presented.

Using the two key components of the CSM – the base curve and the material model, cross-section resistance expressions for axial compression and bending in isolation were presented. Comparisons with test data revealed that the CSM provides closer and more consistent predictions of capacity than existing design codes, through a rational allowance of strain hardening.

Extension of the strain based design from simple axial and bending resistances to the general case of combined loading was then presented. A numerical method was formulated to generate interaction surfaces for box sections and I-sections, by computing all permutations of uniform and linearly varying strains, which when combined did not exceed the CSM limiting strain in compression. From the numerical results, design expressions to describe the interaction surfaces, anchored to the CSM end-points, were developed, with the key parameters determined by means of non-linear least squares regression. The accuracy of the fits to the numerical model envelopes was assessed through a residual analysis, which showed excellent agreement with deviations of less than 3.5%. Use of the EN 1993-1-1 interaction curves, but with CSM end-points, also yielded accurate results. Comparisons of the resulting design expressions were then made with tests, which showed similarly good agreement to that observed under the individual load cases.

REFERENCES

[1] EN 1993-1-1. Eurocode 3: design of steel structures — part 1-1: general rules and rules for buildings *European standard*, CEN: 1–96, (2005)
[2] BS 5950-1. Structural use of steelwork in buildings — part 1 *British standard*, BSI (2000)
[3] R. Greiner, M. Kettler, A. Lechner, B. Freytag, J. Linder, J.P. Jaspart, *et al*. Plastic member capacity of semi-compact steel sections — a more economic design Eur Res Fund Coal Steel (2008)
[4] P. JuhásElastic–plastic bending load-carrying capacity of steel members Challenges, opportunities and solutions in structural engineering and construction (2010), pp. 141–147
[5] Y. Shifferaw, B.W. Schafer Inelastic bending capacity of cold-formed steel members
[6] J Sruct Eng ASCE, 138 (4) (2012), pp. 468–480
[7] A.R. Kemp, M.P. Byfield, D.A. Nethercot Effect of strain hardening on flexural properties of steel beams
[8] Struct Eng, 80 (8) (2002), pp. 188–197

AUTHOR PROFILE

Jyoti B.Tech., M. Tech. Scholar in Civil Engineering (Structural Design) from Ganga Institute of Technology and Management, Kablana, Jhajjar, Haryana (India) affiliated to Maharshi Dayanand University, Rohtak, Haryana (India).